

REMARKS/ARGUMENTS

Claims 1-20 are pending, claims 14-19 having been withdrawn from consideration. By this Amendment, claims 1, 2, 5-13 and 20 are amended. Support for the amendments to claims 1, 2, 5-13 and 20 can be found, for example, in original claims 1, 2, 5-13 and 20. No new matter is added. In view of the foregoing amendments and following remarks, reconsideration and allowance are respectfully requested.

Allowable Subject Matter

Applicants thank the Examiner for the indication in the Office Action that claims 3 and 12 recite allowable subject matter.

Withdrawn Claims

For the reasons set forth below, Applicants submit that all pending claims presently subject to examination are in condition for allowance. Because withdrawn claims depend from, and thus recite all features of, allowable claims, rejoinder and allowance of the withdrawn claims are respectfully requested.

Rejection Under 35 U.S.C. §112, Second Paragraph

The Office Action rejects claims 9 and 20 as indefinite under 35 U.S.C. §112, second paragraph. By this Amendment, claims 9 and 20 are amended to obviate the rejection. Accordingly, reconsideration and withdrawal of the rejection are respectfully requested.

Rejection Under 35 U.S.C. §103

The Office Action rejects claims 1, 2, 4-11, 13 and 20 under 35 U.S.C. §103(a) over Takahashi et al., ("Photocatalytic properties of TiO₂/WO₃ bilayers ..." 2003) ("Takahashi") in

view of Zeman et al. ("Nano-scaled photocatalytic TiO₂ ..." 2003) ("Zeman"), Zhang et al. ("Surface modification of TiO₂ film by iron doping ..." 2003) ("Zheng") and U.S. Patent No. 6,576,344 to Doushita et al. ("Doushita"). Applicants respectfully traverse the rejection.

Claim 1 recites "[a] structure, comprising: a substrate; and an antisoiling layer having a photocatalytic property formed on at least part of a surface of the substrate; wherein: the antisoiling layer comprises a titanium dioxide-based layer and an underlayer (UL) immediately beneath the titanium dioxide-based layer; the titanium dioxide-based layer comprises titanium oxide at least partly crystallized in anatase form; the underlayer (UL) has a crystallographic structure that assisted in crystallization of the titanium oxide, by heteroepitaxial growth in the anatase form, of the titanium oxide-based layer; and the photocatalytic property is obtained without performing a heating step" (emphasis added). Takahashi, Zeman, Zheng and Doushita do not disclose or suggest such a structure.

As indicated above, the structure of claim 1 requires a titanium oxide layer at least partly crystallized in anatase form and an underlayer having crystallographic structure that assists in crystallization of the titanium oxide by heteroepitaxial growth. Takahashi is an academic study of TiO₂/WO₃ bilayers formed on glass substrates. *See Takahashi*, Abstract, page 1410. However, Takahashi does not disclose a structure as recited in claim 1.

At the outset, there is no disclosure in Takahashi that the employed TiO₂ layer is anatase TiO₂. Moreover, one could not assume based on the disclosure of Takahashi that the employed TiO₂ layer is necessarily formed of anatase TiO₂ because the disclosed bilayer has photocatalytic properties. One of ordinary skill in the art would readily appreciate that other crystalline forms of TiO₂, such as rutile TiO₂, may exhibit photocatalytic activity. *See* MPEP §2112.IV (citing *In re Rijckaert*, 9 F.3d 1531 (Fed. Cir. 1993) ("[t]he fact that certain result or characteristic may occur or be present in the prior art is not sufficient to establish the

inherency of the result or characteristic"). Thus, Takahashi does not explicitly or inherently disclose employing anatase TiO₂ in the described bilayer.

Takahashi also does not disclose the underlayer of claim 1. As indicated above, the underlayer of claim 1 has a crystallographic structure that assists in crystallization of the titanium oxide by heteroepitaxial growth. Such epitaxy is possible when there is some similarity between the crystallographic structure of the coating and the material that is coated, particularly in terms of lattice parameters. Applicants have attached an article for reference, Takahashi et al., "Influence of working gas pressure on structure and properties of WO₃ films reactively deposited by rf magnetron sputtering," J. Vac. Sci. Technol. A 21(4), July/Aug 2003 ("Takahashi II").

Takahashi II describes forming WO₃ layers in the same manner as described in preparation of the WO₃ layer of the bilayer of Takahashi. Takahashi II discloses that the described WO₃ layer is monoclinic with crystallographic axis c perpendicular to the substrate. *See* Takahashi II, pages 1415 to 1416. Monoclinic WO₃ has the following lattice parameters: a = 0.7297 nm, b = 0.7539 nm and c = 0.7688 nm. By contrast, anatase TiO₂ has a tetragonal structure where: a = 0.3784 nm and c = 0.9515 nm. In view of these dramatic differences in lattice parameters, one of ordinary skill in the art would understand that the WO₃ under layer of Takahashi does not promote the heteroepitaxial growth of anatase TiO₂. The WO₃ layer of Takahashi is not an underlayer as recited in claim 1.

Moreover, Applicants note that Takahashi does not indicate that the WO₃ underlayer in the described bilayer could or should be used to promote growth of anatase TiO₂. Rather, Takahashi indicates that the underlayer is selected to promote photocatalytic activity induced by visible light. *See* Takahashi, page 1414. There is nothing in Takahashi (or the other cited references) that would have led a skilled artisan to modify the disclosed bilayer to replace the

WO₃ layer with a layer having crystallographic structure that assists in crystallization of the anatase titanium oxide by heteroepitaxial growth, as recited in claim 1.

For the reasons discussed above, Takahashi fails to disclose or suggest each and every feature of claim 1. Zeman, Zheng and Doushita do not remedy the deficiencies of Takahashi. Zeman is cited for its alleged disclosure of employing magnetron sputtering to form titanium oxide films. *See* Office Action, page 5. Zheng is cited for its alleged disclosure of doping a titanium oxide film with iron. *See* Office Action, page 6. Doushita is cited for its alleged disclosure of forming a anti-soiling titanium oxide layer over a glass substrate having an alkali-blocking film *See* Office Action, page 6. However, like Takahashi, none of Zeman, Zheng and Doushita discloses or suggests a titanium oxide layer at least partly crystallized in anatase form and an underlayer having crystallographic structure that assists in crystallization of the titanium oxide by heteroepitaxial growth. Accordingly the combination of references fails to disclose or suggest each and every feature of claim 1.

As explained, claim 1 would not have been rendered obvious by Takahashi, Zeman, Zheng and Doushita. Claims 2, 4-11, 13 and 20 depend from claim 1 and, thus, also would not have been rendered obvious by Takahashi, Zeman, Zheng and Doushita. Accordingly, reconsideration and withdrawal of the rejection are respectfully requested.

Conclusion

For the foregoing reasons, Applicants submit that claims 1-20 are in condition for allowance. Prompt reconsideration and allowance are respectfully requested.

Respectfully submitted,

OBLON, SPIVAK, McCLELLAND,
MAIER & NEUSTADT, P.C.

Norman F. Oblon

Jacob A. Doughty
Registration No. 46,671

Customer Number

22850

Tel: (703) 413-3000
Fax: (703) 413 -2220
(OSMMN 08/07)

Attachment:

Takahashi et al., "Influence of working gas pressure on structure and properties of WO₃ films reactively deposited by rf magnetron sputtering," J. Vac. Sci. Technol. A 21(4), July/Aug 2003

Influence of working gas pressure on structure and properties of WO_3 films reactively deposited by rf magnetron sputtering

T. Takahashi,^{a)} J. Tanabe, N. Yamada, and H. Nakabayashi

Department of Electrical and Electronic Engineering, Faculty of Engineering, Toyama University,
3190 Gofuku, Toyama 930-8555, Japan

(Received 23 October 2002; accepted 17 March 2003; published 2 July 2003)

Tungsten trioxide (WO_3) films with thickness of 0.9–6.7 μm have been deposited on glass-slide substrates, using rf magnetron sputtering in an atmosphere of mixture 80% Ar and 20% O_2 . The as-deposited films had a dark metallic color, like the W target, at a working gas pressure P_W of 1 mTorr. Yellow films resulted at a P_W of 3 mTorr. With a further increase of P_W , the film color changed to pale yellow. From the x-ray diffraction patterns, the as-deposited films were polycrystalline crystallizing in the monoclinic crystal structure with high *c*-axis orientation perpendicular to the film plane. The optical transmittance of the films deposited at a P_W of 1 mTorr is nearly zero. However, the transmittance of the films deposited at other P_W are larger than 70% in the wavelength, λ , ranging from 500 to 900 nm. With decreasing λ to 400 nm, the transmittance decreases steeply to zero. The λ at this absorption edge is longer than that in TiO_2 and comes in the visible region. The surface morphology of the films depends on P_W . This different morphology may be attributed to the effect of the substrate heating by plasma emission because of the high plasma density at higher P_W . The morphology of the films may also depend on the crystallinity of the WO_3 films. As P_W increased, the surfaces of the films became rougher but the grain sizes of the films did not always become larger. The WO_3 films deposited in this study may be used for the underlayer of TiO_2 photocatalyst. © 2003 American Vacuum Society. [DOI: 10.1116/1.1575216]

I. INTRODUCTION

Tungsten trioxide (WO_3) has been studied by many researchers because of its semiconductive nature and electrochromic properties.¹ Recently, the physicochemical properties of the WO_3 materials were used for photocatalysis research because its band gap, E_g , is suitable for the solar spectrum.^{2–4} The band gap of WO_3 is between 2.7–2.8 eV.^{5,6} The wavelength λ at the optical adsorption edge shifts in the range of 413 to 477 nm corresponding to E_g in the range of 3 to 2.6 eV.⁷ The surface coloration of the WO_3 compound semiconductor with monoclinic crystal structure at 298 K changes from yellow to green with increasing the oxygen deficiency in the compound composition.⁷ It has been reported that the photoproduction of oxygen and hydrogen has been successfully performed using an aqueous suspension containing WO_3 , Fe^{2+} , and Fe^{3+} species.⁷

In photocatalysis studies, a TiO_2 photocatalyst can only react slightly to solar energy because it has an E_g smaller than 3.2 eV (λ of 380 nm). So, it is desirable for most solar energy applications to have new materials that can react strongly to visible light. Therefore, the WO_3 semiconductors with suitable E_g are very useful as composite materials for a TiO_2 photocatalyst.

A TiO_2 photocatalyst has mainly been prepared as a film in a form in wide general use, by various methods, such as rf reactive ion plating, metalorganic decomposition, metal organic chemical vapor deposition, thermal oxidation of Ti sputtered films, rf reactive magnetron sputtering, metal ion implantation of TiO_2 film, and sol-gel thin film.⁸ Therefore,

WO_3 is a very suitable semiconductor on which to deposit TiO_2 . WO_3 films have been deposited by various techniques, such as rf sputtering from a compressed powder WO_3 target,⁹ dc reactive sputtering from a metallic tungsten target,¹⁰ thermal evaporation from large-grained water-free WO_3 ,¹¹ and oxidation of reflective tungsten films.¹²

In this study, the WO_3 films for an underlayer of a TiO_2 photocatalyst have been deposited using conventional magnetron sputtering with rf power in an atmosphere of 80% Ar-20% O_2 . The crystallographic and surface structures and the optical properties of WO_3 films deposited under different preparation conditions have been investigated in detail. Gaseous methyl alcohol, having an easy and fundamental decomposition to analyze in organic chemistry, has also been studied in order to investigate the photocatalytic effects of the WO_3 underlayer.

II. EXPERIMENTAL PROCEDURE

WO_3 films have been prepared in an rf magnetron sputtering apparatus at room temperature. Figure 1 shows the schematic illustration of the sputtering apparatus used in this study. A tungsten (W) disk with 120 mm diameter, 3 mm thickness, and purity of 99.9%, and glass-slides were used as a target, and substrates, respectively.

WO_3 films of thickness 0.9–6.7 μm have been deposited in order to investigate the influence of the working gas pressure on crystal structure, optical properties, and surface morphology. The sputtering was carried out after evacuating to a background pressure below 3×10^{-6} Torr and working gas pressures of P_W : 1–8 mTorr were used (80:20; Ar: O_2 mixture).

^{a)}Electronic mail: takahashi@eng.toyama-u.ac.jp

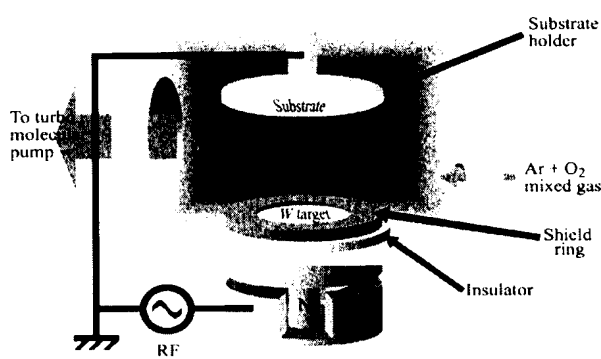


FIG. 1. Schematic illustration of rf magnetron sputtering apparatus used in this study.

The sputtering conditions are listed in Table I. The film thickness δ was measured with a mechanical surface roughness gauge using the step between film and substrate. The crystal structures, optical properties, and surface roughness of the WO_3 films were determined by x-ray diffraction analysis with $\text{Cu}-K\alpha$, a spectrophotometer and atomic force microscopy (AFM), respectively. These measurements were mostly carried out at room temperature.

III. RESULTS AND DISCUSSION

When the WO_3 films were deposited at a P_W of 1 mTorr, the surfaces of films had high conductivity and a metallic color, like the W target. This may be attributed to the insufficient oxidation of the tungsten owing to reduced oxygen in the as-deposited films. The WO_3 films deposited at a P_W of 3 mTorr were yellow and with further increase of a P_W above 3 mTorr, the surface coloration of the WO_3 films became pale yellow. The surface coloration of the high-purity powdered WO_3 changes from yellow to greenish because of an increase of the oxygen deficiency.⁷ The composition near the surface of the WO_3 film was investigated by qualitative analysis using Auger electron spectroscopy. The oxygen content in the films gradually became higher with increasing P_W , while the WO_3 films showing the surface yellow had the highest oxygen content. However, the atomic ratio of

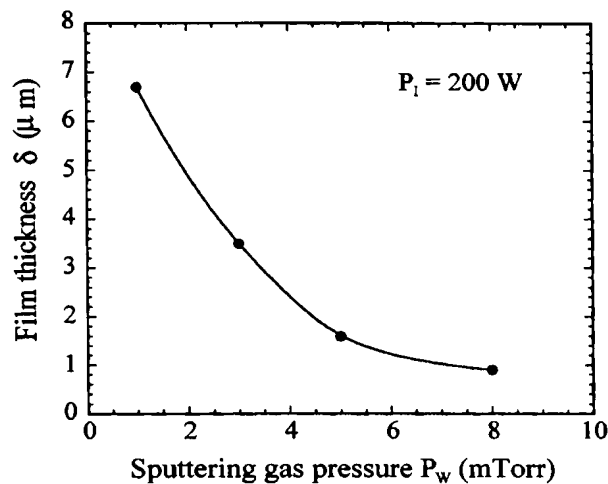


FIG. 2. Relationship between the film thickness δ of the as-deposited WO_3 films and the working gas pressure P_W .

W/O could not be estimated with accuracy because of the oxygen adsorbed onto the film surface. The surface coloration of WO_3 films deposited in this study may be due to the change of the film composition as well as the powdered WO_3 in JCPDS-International Center for Diffraction Data.

Figure 2 shows the relationship between the film thickness δ and the working gas pressure P_W . The film thickness δ decreased steeply from 6.7 to 3.5 μm with increasing P_W in the range of 1 to 3 mTorr. Then δ decreased gradually from 3.5 to 0.9 μm with further increase of P_W . The WO_3 films deposited at P_W of 1 mTorr have a large film thickness corresponding to the deposition rate of 111.7 nm/min. This deposition rate can be obtained in the deposition of metallic tungsten. When a P_W is higher than 1 mTorr, the deposition rates of the WO_3 films significantly decrease because of the enhancements of the oxidation of the tungsten and the collision between sputtered atom and gas molecular, as compared at a P_W of 1 mTorr.

Figure 3 shows the x-ray diffraction patterns at various P_W . From the x-ray diffraction pattern, the WO_3 films deposited at a P_W of 1 mTorr had no clear peaks and the structures were amorphous. As P_W increases, the as-deposited films were polycrystalline with a monoclinic form, and the

TABLE I. Sputtering conditions.

Background pressure	P_{BG}	$\sim 3 \times 10^{-6}$ Torr
Target	W disk plate Diameter 120 mm, thickness 3 mm, purity 99.9%	
Substrate	Glass-slide substrate	
rf input power	P_1	200 W
Working gas pressure	P_W	1–8 mTorr
Target–substrate distance	D_{T-S}	50 mm
Ratio of gas composition	G_R	Ar:O ₂ = 4:1
Sputtering time	t_S	60 min
Deposition rate	R_D	15–111.7 nm/min
Film thickness	δ	900–6700 nm

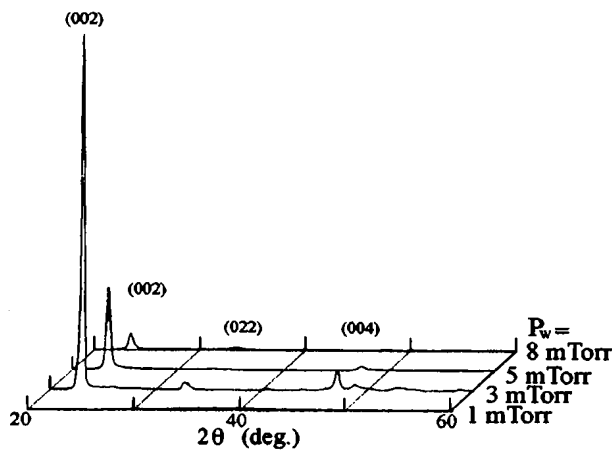


FIG. 3. X-ray diffraction patterns of the as-deposited WO_3 films at various P_w .

(001) crystallographic plane was predominantly oriented parallel to the film plane, that is, the crystallographic axis of c was perpendicular to the film plane. However, as the weak peak lines of (022) crystallographic plane were also observed in the films deposited at a P_w of 3 and 8 mTorr, the crystallographic structure of the films does not show a uniaxial orientation perpendicular to the film plane. In this study, the best preparation condition with a good crystallinity predominantly oriented (001) plane was P_w of 3 mTorr. This result shows a similar tendency to the WO_3 polycrystalline films prepared by oxidation of reflective tungsten films.¹² The crystallite size $\langle D_{(001)} \rangle$ was calculated by the full width at half maximum of the (001) peak in the x-ray diagrams. The obtained data of $\langle D_{(001)} \rangle$ are 23, 17, and 15 nm at P_w of 3, 5, and 8 mTorr, respectively. The $\langle D_{(001)} \rangle$ decreased with an increase of P_w . It has been found that the crystallographic structure of the films significantly depended on the working gas pressure.

Figure 4 shows the optical transmittance spectra at vari-

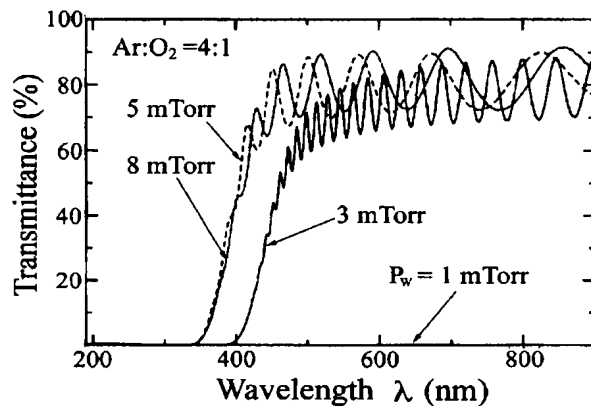


FIG. 4. Optical transmittance spectra of the as-deposited WO_3 films at various P_w .

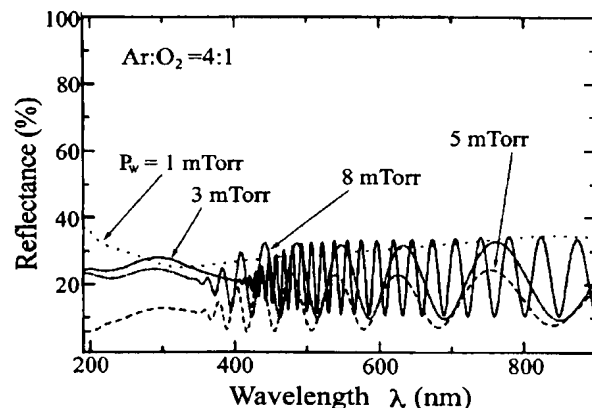


FIG. 5. Reflectance spectra of the as-deposited WO_3 films at various P_w .

ous P_w . The optical transmittance of the films deposited at P_w of 1 mTorr is nearly zero. This may due to the metallic film of a characteristic spectrum with the reflectance and adsorption of the light. However, the transmittance of the films deposited at P_w of 3 mTorr is about 80% in the wavelength λ ranging from 500 to 900 nm. The transmittance steeply decreases with decreasing λ ranging from 500 to 400 nm. And then, the transmittance becomes zero at λ of 380 nm. This is a longer wavelength than that of TiO_2 . At a P_w higher than 3 mTorr, the transmittance of the films is about 90% in the wavelength λ ranging from 400 to 900 nm. The transmittance steeply decreases with further decrease of λ . And then the transmittance becomes zero at λ of 340 nm. This is the same wavelength as that of TiO_2 .

These results show a similar tendency to the rf sputtered films⁹ and reactively dc sputtered WO_3 films.¹⁰ However, the adsorption edge shifts to a longer wavelength at a P_w of 3 mTorr. This may be due to the good crystallinity. It has been found that the working gas pressure successfully controlled the optical transmittance of the films.

Figure 5 shows the reflectance spectra at various P_w . The optical reflectance of the films deposited at a P_w of 1 mTorr is a constant value of about 35% in the wide range of the wavelength. This may be due to the metallic films. In the films deposited at a P_w higher than 1 mTorr, the optical reflectance ranging from 10% to 35% shows a similar tendency regardless of the working gas pressure.

The clusters bonding the spherical grains appeared in most films. The metallic films deposited at a P_w of 1 mTorr have very smooth surface with the spherical grains of a diameter of approximate 10–20 nm. In the WO_3 film deposited at a P_w of 3 mTorr, the spherical grains of a diameter of approximate 60–100 nm was observed and larger clusters bonding the spherical grains appeared. The size of the spherical grain gradually became smaller with a further increase of P_w . The spherical grain size was approximately 60–80 nm at a P_w of 8 mTorr. AFM images indicate that the surface morphology of WO_3 films strongly depends on P_w . This different morphology may be attributed to the effect of the substrate heating by plasma emission because of the high

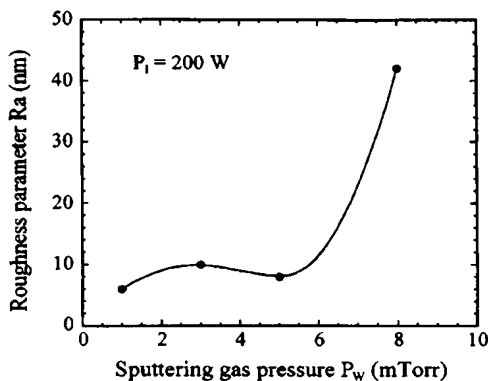


FIG. 6. Relationship between the roughness parameter R_a of the as-deposited WO_3 films and P_w .

plasma density at a higher P_w . The morphology of the films may also depend on the crystallinity of the WO_3 films.

In order to evaluate the quantitative analysis of the surface roughness, the roughness parameter R_a was evaluated by use of the following equation:¹³

$$R_a = \frac{1}{L} \int_0^L |Z_0 - Z(x)| dx,$$

where Z_0 is an average height over the interval from 0 to L in x , which covers the 125 nm square area in parallel with the substrate, and $Z(x)$ is the height of the film surface at position x .

Z_0 can be expressed as:

$$Z_0 = \frac{1}{L} \int_0^L Z(x) dx.$$

Figure 6 shows the relationship between the roughness parameter R_a of the WO_3 films and P_w . The R_a of the films deposited at a P_w in the range of 1 to 5 mTorr has a constant value of about 7 nm. Then, the R_a rapidly increases to 42 nm with a further increase of P_w . This result may be attributed to the difference of the bombarding energy of charged particles to the growing films and the substrates.

In order to confirm the photocatalytic reactions of the TiO_2/WO_3 bilayers, the gaseous methyl alcohol has been decomposed under irradiation with artificial sunrays of wavelength λ ranging from 330 to 750 nm for 130 min at room temperature. The various products of decomposed gaseous methyl alcohol were analyzed with a Fourier transform infrared (FTIR) spectrophotometer.

TiO_2 films with a thickness of about 1.4 μm were deposited onto the as-deposited WO_3 films using dc sputtering at a working gas pressure P_w of 1 mTorr, and a mixed Ar/O₂ atmosphere with 10 and 5 sccm flow.^{8,14}

Figure 7 shows the time dependence of the photocatalytic decomposition of CH_3OH into CO_2 and H_2O on the TiO_2/WO_3 bilayers under irradiation with artificial sunlight, where the WO_3 layer was deposited at a P_w of 3 mTorr. Also

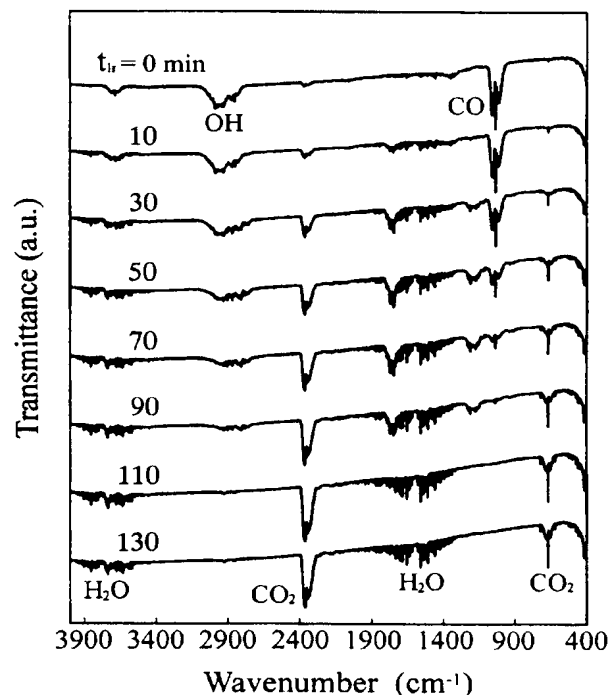


FIG. 7. Time dependence of the photocatalytic decomposition of CH_3OH into CO_2 and H_2O on the TiO_2/WO_3 bilayers under irradiation with artificial sunrays, where WO_3 layer was deposited at a P_w of 3 mTorr.

shown in Fig. 7 are typical experimental results of the strongest photocatalytic decompositions. In Fig. 7, when the irradiation time is zero, the adsorption peaks corresponding to the existence of OH radicals clearly appeared at a wave number of 1200 cm^{-1} and 2900 cm^{-1} as well as TiO_2 monolayers. Then, with increasing the irradiation time, the adsorption peaks corresponding to the vibration of CO_2 molecules were apparently observed at wave numbers of 667 cm^{-1} and 2349 cm^{-1} . The adsorption peaks of 1600 and 3800 cm^{-1} show the vibration of H_2O molecules. The adsorption peak at wave numbers of 1030 cm^{-1} and 2940 cm^{-1} may be due to the stretching vibration of CO , and OH radicals, respectively. The CO and OH peaks became lower, while the CO_2 and H_2O peaks became higher with increasing irradiation time. The ability of the gas decomposition is larger than that in TiO_2 monolayers. This depends on the optical transmittance spectra and the thickness of the bilayers. As the thickness of the bilayer is thicker than that of the monolayer, the much visible light may be adsorbed within the bilayers.

Figure 8 shows the relationship between the peak height of 2349 cm^{-1} in the FTIR transmittance spectra of as-deposited TiO_2/WO_3 bilayers and the irradiation time t_{IR} : Various P_w for depositing the WO_3 bilayers, and the data of the TiO_2 monolayer are shown. The peak height increased with increasing t_{IR} regardless of P_w . The degree of an increase of the peak height is larger with decreasing P_w . In t_{IR} of 130 min, the peak heights of the bilayers at a P_w of 3 mTorr are about two times as much as that in the TiO_2 mono-

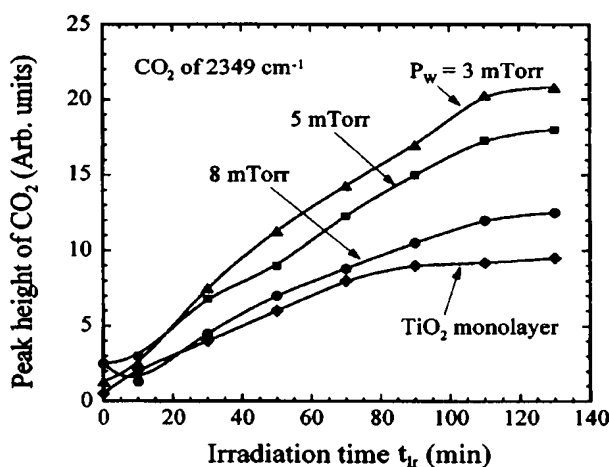


FIG. 8. Relationship between the peak height of 2349 cm^{-1} in the FTIR transmittance spectra of the TiO_2/WO_3 bilayers and the sunray irradiation time t_{ir} as a parameter of P_w for depositing the WO_3 films.

layer. The CH_3OH can more easily be decomposed into CO_2 and H_2O molecules as compared to the TiO_2 monolayer. The activity of the decomposition of CH_3OH may depend on the crystallinity and optical properties of WO_3 layers.

IV. CONCLUSION

WO_3 films with thickness of 0.9–6.7 μm have been deposited on glass-slide substrates, using rf magnetron sputtering in an atmosphere of mixture 80% Ar and 20% O_2 . The crystal structure and the surface morphology and the optical properties of WO_3 films deposited at the working gas pressure P_w ranging from 1 to 8 mTorr have been investigated.

The as-deposited films had dark metallic color, like the W target at a P_w of 1 mTorr. When the films were deposited at P_w of 3 mTorr, the surface coloration of the WO_3 films became yellow. With a further increase of P_w , the surface color changed to pale yellow. From the x-ray diffraction pat-

terns, the as-deposited films were shown to be polycrystalline, crystallizing in the monoclinic crystal structure with the high c -axis orientation perpendicular to the film plane. The optical transmittance of the films deposited at a P_w of 1 mTorr is nearly zero. However, the transmittance of the films deposited at other P_w are larger than 70% in the wavelength λ ranging from 500 to 900 nm. On decreasing λ to 400 nm, the transmittance falls steeply to zero. The λ at this absorption edge is longer than that in TiO_2 and comes in the visible region. The surface morphology of the films depends on P_w . The WO_3 films deposited in this study may be used as the underlayer of TiO_2 photocatalyst.

ACKNOWLEDGMENTS

The authors would like to thank Professor N. Nakatani and Associate Professor T. Yamazaki of Toyama University for spectrophotometer measurements. This work was supported by a Grant-in-Aid for Scientific Research from the Japan Society for the Promotion of Science.

- ¹S. Sawada and G. C. Danielson, Phys. Rev. **113**, 1008 (1959); M. J. DeVries, C. Trimble, T. E. Twald, D. W. Thompson, J. A. Woollam, and J. S. Hale, J. Vac. Sci. Technol. A **17**, 2906 (1999).
- ²D. E. Scaife, Sol. Energy **25**, 41 (1980).
- ³W. Erbs, J. Desilvestro, E. Borgarello, and M. Gratzel, J. Phys. Chem. **88**, 4001 (1984).
- ⁴J. Desilvestro and M. Neumann-Spallart, J. Phys. Chem. **89**, 3684 (1985).
- ⁵M. T. Nenadovich, T. Rajh, O. I. Micic, and A. J. Nozik, J. Phys. Chem. **88**, 5827 (1984).
- ⁶H. P. Maruska and A. K. Ghosh, Sol. Energy **20**, 445 (1978).
- ⁷G. R. Bamwenda, K. Sayama, and H. Arakawa, J. Photochem. Photobiol., A **122**, 175 (1999).
- ⁸T. Takahashi, H. Nakabayashi, and W. Mizuno, J. Vac. Sci. Technol. A **20**, 1916 (2002).
- ⁹H. Kaneko, S. Nishimoto, K. Miyake, and N. Suedomi, J. Appl. Phys. **59**, 2526 (1986).
- ¹⁰H. Kaneko, F. Nagao, and K. Miyake, J. Appl. Phys. **63**, 510 (1988).
- ¹¹T. J. Tate, M. Garcia-Parajo, and M. Green, J. Appl. Phys. **70**, 3509 (1991).
- ¹²D. Davazoglou and A. Donnadieu, J. Appl. Phys. **72**, 1502 (1992).
- ¹³T. Takahashi, H. Nakabayashi, T. Terasawa, and K. Masugata, J. Vac. Sci. Technol. A **20**, 1205 (2002).
- ¹⁴T. Takahashi and H. Nakabayashi, Thin Solid Films **420-421**, 433 (2002).